International Journal of Applied Pharmaceutics

ISSN- 0975-7058 Vol 15, Issue 3, 2023

Original Article

FORMULATION AND DEVELOPMENT OF GALLEN GUM LOADED SELF-ASSEMBLED MIXED MICELLES SYSTEM BASED ON FLAVONOID PHOSPHOLIPID COMPLEX

MANJUSHA A. BHANGE[1*], ANIL M. PETHE[1], AMRAPALI JADHAV[2], HARSHADA KANADJE[3]

[1*]Department of Pharmaceutics, Datta Meghe College of Pharmacy, DMIHER (DU), Sawangi, Wardha-442001, Maharashtra, India. [2]Department of Pharmaceutics, Government College of Pharmacy, Aurangabad, Maharashtra, India. [3]Department of Pharmaceutical Quality Assurance, DBSS's Rajarshi Shahu College of Pharmacy, Buldana, Maharashtra, India
Email: manjubhange@gmail.com

Received: 24 Oct 2022, Revised and Accepted: 22 Feb 2023

ABSTRACT

Objective: Research on the development of pharmaceutical self-assembled mixed micells systems is in that they have the advantage of keeping the drug's encapsulating qualities while also enhancing its physicochemical characteristics. The goal of this study was to make the class II biopharmaceutical quercetin more soluble in water and more bioavailable when taken orally (QCT). The enhancement of encapsulation and flavonoids loading within mixed micelles using solvent evapouration technique.

Methods: In the present study, pharmaceutical mixed micells of a BCS class II drug, QCT were prepared using solvent evapouration technique method. Prepared mixed micells were characterized using Critical micelle concentration (CMC), Fourier Transform Infrared (FT-IR), Particle size and zeta potential, Powder X-Ray Diffract meter (PXRD), *In vitro* dissolution, Transmission electron microscopy (TEM). In addition *In vitro* drug release studies were also performed.

Results: The results of the characterization studies indicated the designing of gallen gum loaded self-assembled mixed micelles system based on flavonoid phospholipid complex. The CMC of LS-75 and LS-100 binary mixture had shows good results to be 0.0013%. The FTIR spectra of complex showed characteristic peak of QCT shows abundant effect on O-H (aromatic), C-O (aromatic), C-C, and aromatic C-O is observed at 3282.2, 1620.1, 1058.7, and 1162.2 respectively. The average particle size of design-optimized quercetin mixed micells (QCT-MMs) was demonstrated to be ~116.1 nm, as evaluated by Malvern. From the obtained particle size, it indicated that the particle size of QCT in QCT-MMs was widely distributed. The polydispersity index (PDI) for QCT-MMs was found in the range of ~ 1.000, zeta potential value for QCT-MMs as evaluated by Malvern was observed to be ~-99.2 mV. The P-XRD, SEM, showed good powder diffraction results with having good flow property. Also formulation were evaluated for the *In vitro* drug dissolution study for rate of extent of drug release and dissolution rate release of QCT from QCT-MMs was sustained up to 72 h. TEM images of QCT-MMs, where the micelles exhibited relatively regular dark stained shapes appearing more or less spherical or spheroid.

Conclusion: It can be concluded that the QCT-MMs enhance the aqueous solubility of the QCT and increased the bioavailability and retention time.

Keywords: QCT, Phospholipids S-75, Phospholipid S-100, Solvent evapouration method, Mixed micells

DOI: https://dx.doi.org/10.22159/ijap.2023v15i3.46795. Journal homepage: https://innovareacademics.in/journals/index.php/ijap

INTRODUCTION

Micellar amphiphile compositions for drug delivery are successful. Due to the hydrophobic core of micelles, water-insoluble drugs can be easily solubilized and delivered [1]. Targeted drug delivery systems reduce drug degradation and loss, limit side effects, promote medication bioavailability, and increase the number of medicines at the zone of interest [2]. Drug carriers include soluble and insoluble polymers, microparticles, cells, cell ghosts, lipoproteins, liposomes, and amphiphilic polymer-based micellar systems. Globally, people get cancer. Uncontrolled, uncoordinated, unfavorable cell division characterizes it. Cancer cells continue to divide and move through the blood and lymph systems, unlike normal cells [3]. When faulty cells don't die and new cells form when the body doesn't need them, they can create a malignant tumor or neoplasm. Mutations can affect normal cell development and division if cells' DNA is damaged or altered. The major cause of cancer death is metastasis [4].

National Cancer Institute (NCI) and WHO anticipates that 1.9 million men and women will be diagnosed with all cancers at some time in their life. Comparatively, there were enough cancer-related deaths [5]. Lung, liver, stomach, colorectal, and breast cancers are the most deadly. High BMI, inadequate fruit and vegetable intake, lack of exercise, and cigarette and alcohol use cause 81% of cancer fatalities [6]. Cancer treatments include surgery, chemotherapy, radiation, immunotherapy, and monoclonal antibody therapy. The sort of therapy chosen depends on the tumor's location, grade, stage, and the patient's condition [7]. In cancer patients, physiological changes resulted in negative energy balance, growth standstill, and weight loss. In other cases, such as gastrointestinal difficulties, the cause of decreased intake may be clear [8]. Higher energy consumption in cancer patients involves both tumor and host energy demands [9]. The tumor's glucose and protein metabolism will be detailed below. Tumor blood flow may increase heart energy use. Energy expenditure increases oxygen intake and carbon dioxide production, which may increase breathing work [10].

Conventional chemotherapy has medication delivery problems. Particle size, content, and surface charge affect drug transport. Pathophysiological tumor heterogeneity inhibits uniform drug delivery throughout the tumor [11]. The acidic tumor microenvironment destroys acid-sensitive medications [12]. Most medicines are given orally. The bioavailability pharmacokinetics profile of an orally administered drug depends on solubility in water [13]. Oral administration is the most common route due to patient compliance and reduced manufacturing costs. Limited bioavailability is a hurdle to oral dose formulations. Poor bioavailability is due to low aqueous solubility and plasma membrane permeability [13-15].

In the present study developed QCT-MMs using was selected as the Phospolipid S-100 and phospholipid S-75 carrier and employed in the micells formulations at various drug/phospholipid ratios. The QCT-MMs was characterized for CMC, FTIR, particle size and zeta potential, PXRD, *in vitro* drug dissolution study.

MATERIALS AND METHODS

Quercetin was gifted by Yucca Enterprises, Mumbai India. Lipoid S-75, Lipoid S-100, by Ludwigshafen, Germany. Ethanol (Absolute), Tween 80, Di chloro methene, and Acetonitrile Iodine was purchased from Ozone® International, Ahmedabad, India.

Preparation of the drug drug-loaded mixed micelles

QCT-MMs solution was prepared by Thin Film Hydration method. Measured quantities of Quercetin, Phospholipids S-75 and were dissolved in a 10 ml ethanol (1:1). The solution was sonicated for 1h. Then after 1hr add Phospolipid S-100 to the solution and attached the flask to the rotary vacuum evaporator. The solvent was removed entirely by rotary vacuum evaporation under 45 °C (±5 °C) to form a homogeneous and transparent film. The resulting film was dissolved in 10 ml of the dispersion medium [16, 17]. The obtained solution was mixed with 2 % w/v D-mannitol and was then lyophilized using a lyophilizer under-80 °C for 72 h. The lyophilized QCT-MMs were reconstituted by ultrapure water when it was used [18].

Physico-chemical characterization

Determination of critical micelle concentration (CMC)

To determine the CMC of QCT-MMs in distilled water, the iodine UV spectroscopy method was used as previously reported (Gaisford *et al.* 1995, 1997). The KI/I2 standard solution was prepared by dissolving 0.5 g of iodine and 1 g of potassium iodide in 50 ml DI water. Thirty-seven samples of polymer solution with concentrations ranging from 0.00001% to 0.1% were prepared. To each of the Lipoid S-75/S-100 binary mixture (1:2 w/w) solutions, 25 l KI/I2 standard preparation was added. The mixtures were incubated for 12 h in a dark room at room temperature before measurement. The UV absorbance value of varying polymer concentrations at 366 nm was measured using a UV–absorbance vis spectrometer (Shimadzu UV-2401, UV-VIS recording spectrophotometer, Japan). Experiments were performed in triplicate. The absorption intensity was plotted against the logarithm of polymer mass concentration. The CMC values correspond to the concentration of the polymer at which the sharp increase in absorbance is observed [19].

FT-IR

The FT-IR spectra of all the samples, such as pure QCT, Lipoid S-75, Lipoid S-100, and QCT-MMs were recorded on an FT-IR spectrophotometer (Model: FTIR-8300, Shimadzu, Kyoto, Japan) [20].

Particle size and zeta potential

The mean diameter and zeta potential of the QCT-MMs were determined by a zeta sizer (Nano ZS90, Malvern Instruments Ltd., UK). All the measurements were analyzed in triplicate at 25 °C [21].

PXRD

Pure QCT, Lipoid S-75, Lipoid S-100, PM, and QCT-MMs formulation was analyzed to study the comparative crystalline status of these samples using powder X-ray diffractometer (Model: D8 ADVANCE, Bruker AXS, Inc., Madison, WI, USA). The operational procedure for PXRD analysis has been reported previously [22].

***In vitro* dissolution test**

The properties of QCT release from the QCT-MMs were measured by the dialysis method. Briefly, 10 ml of QCT-MMs was placed in a dialysis bag (MWCO: 3500 Da), which was tightened and placed into a bottle filled with 50 ml of dissolution medium (pH 7.4 phosphate buffer containing 0.5 % (w/v) Tween 80). The bottle was placed in a gas bath thermostat oscillator at 37 °C and shaken at 120 rpm over 24 h. Meantime, equivalent QCT and QCT Mesylate dissolved in a trace of methanol were diluted to 10 ml purified water and gone through the same operation with QCT-MMs. At specific time intervals, 1 ml of the sample was taken out for concentration measurement, and an isometric dissolution medium was added to the bottle [23].

TEM

The TEM is similar to an optical microscope. It has a very high resolution, which in the case of lattice images, can be as high as 0.1 nm. As a result, extremely high magnification (close to 1 million times) is possible. TEM is used to investigate very thin sections (less than 60 nm in thickness) through cells and tissues, as well as materials and copies of sample surfaces. TEM analysis of QCT MMs was performed through Hitachi (H-7500) 120 kV Transmission Electron Microscope with a CCD Camera With a 40-120 kV working voltage, this instrument has a resolution of 0.36 nm (point to point) and can magnify objects up to 6 lakh times in High-Resolution mode. They are all included: Electron Diffraction, Tungsten Filament, Low Dose Function, High Contrast Mode, and an aerodynamic appearance. The maximum range of views at x700 with dual picture modes, auto-navigation, the biggest possible field with maximum contrast, and auto pre-irradiation mode are some of the instrument's unique features (APIS). The equipment can be upgraded to an analytical system in the future by adding EELS, EDS, and STEM attachments [24].

RESULTS AND DISCUSSION

Optimization of preparation and characterization of QCT-MMs

QCT-MMs were prepared using ethanol based-solvent evaporation method. Before this experiment, the preliminary solubility analysis was conducted for QCT and LS-75, LS-100. It was found that both of these compounds are lipophilic and show higher solubility in organic solvents. This physicochemical property of QCT was utilized in this study and prepared the phospholipids complex using the solvent evaporation method. The phospholipids complex are lipid-compatible molecular aggregates of drug and/or bioactive phospholipids and their formation is depending upon the complete dissolution of a drug as well as phospholipids in common solvents resulting in the formation of stable phospholipids complex. The solubility problem was overcome by using ethanol as a choice of solvent because of its semipolar nature, a class III solvent with a low toxicity profile, and provides higher solubility for QCT and Polymer. Therefore, based on solubility, ethanol was chosen as an optimal solvent for the preparation of stable QCT-MMs. Following this, the QCT-MMs were loaded into gellan gum and developed gellan gum NPs using the ionic gelation method [25].

CMC

CMC of the micelle-forming compound influences it is *in vitro* and *in vivo* stability and low CMC values of LS-75 and LS-100 binary mixture underlay the high stability of LS-75 and LS-100 mixed micelles in solutions upon dilution. In this study, the formation of micelles was monitored by using iodine as a hydrophobic probe. Solubilised I2 prefers to participate in the hydrophobic microenvironment of lipoid-mixed micelles, causing the conversion of I3− to I2 from the excess KI in the solution to maintain the saturated aqueous concentration of I2. The absorption intensity of I2 has been plotted as a function of polymer concentration in fig. and the CMC of LS-75 and LS-100 binary mixture was determined to be 0.0013%. This is a reasonably low concentration, suggesting their high stability and ability to maintain integrity even upon extreme dilution in the body [26].

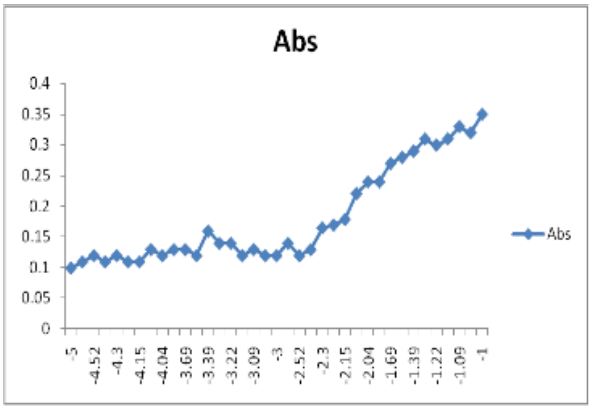

Fig. 1: Plot of UV intensity of I2 vs. concentrations of lipoid S-75/lipoid S-100 in distilled water

FTIR

FT-IR analysis provides vital information about functional group identification and the IR infrared with other components used in the

formulation fig. 2, fig. 3, fig. 4, fig. 5, show the FT-IR spectrum of, Lipoid S-75, Lipoid S-100, QCT, QCT-MMs respectively. The FT-IR spectrum of Lipoid S-75 fig. 2 shows the presence of absorbance peak at~3011.7 (=C-H Stretching), 2922.2 (O-H), 1736.9(C=O Stretching), 1483.5(C=C), 1058.6 (C-O). Lipoid S-100 fig. 3 shows the presence of absorbance peak at~3794 (O-H), 2862 (COOH), 1736.9(C=O Stretching), Furthermore, significant peaks could be detected at 1408Alkane, 1058.6 (CH3) deformation, 1043(C O) vibration, 1733(C=O). Quercetin fig. 4 the major peaks of quercetin. O-H (aromatic), C-O (aromatic), C-C, and aromatic C-O is observed at 3282.2, 1620.1, 1058.7, and 1162.2, respectively. In spectra, all the functional groups of the drug appeared in the QCT-MMs fig. 4 Thus, it was accomplished that there was no interaction of quercetin with the above-mentioned excipients [27, 28].

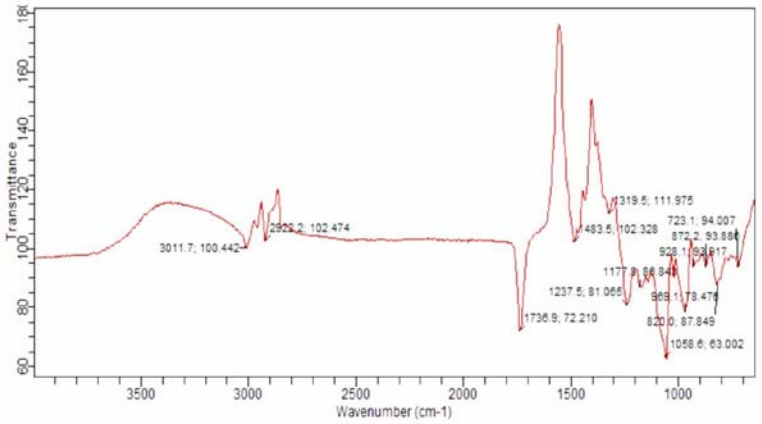

Fig. 2: FT-IR of lipoid S-75

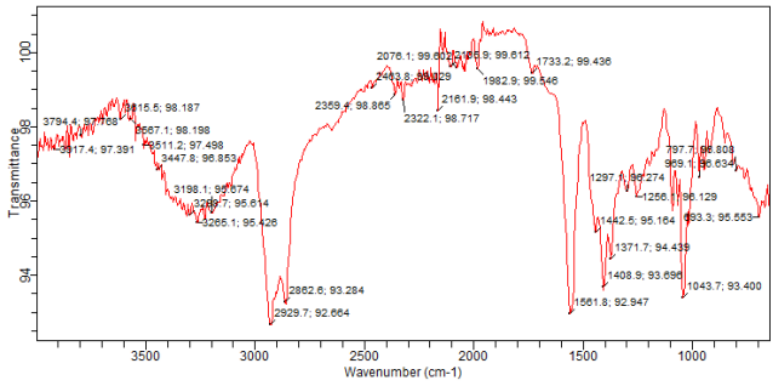

Fig. 3: FT-IR of lipoid S-100

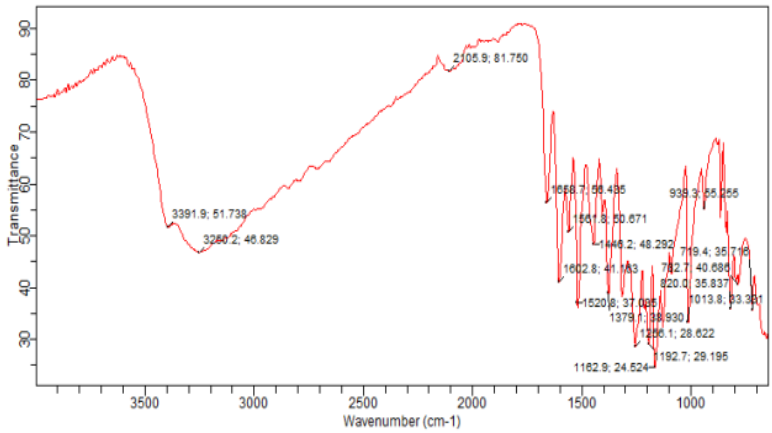

Fig. 4: FT-IR of QCT

The particle size and zeta potential

Particle size distribution and zeta potential are important tools used for the determination of the physical stability of sub-micron particles in the form of a liquid dispersion. Earlier published report on diosmin–phospholipids lyophilized phytosomes exhibited particle size ~536±3.66 nm, found to be suitable for the oral route of administration due to its enhanced aqueous solubility and oral

bioavailability (Freitag *et al.*, 2013). The analyzed particle size distribution of prepared QCT-MMs is shown in fig. 6. The average particle size of design-optimized QCT-MMs was demonstrated to be ~116.1 nm, as evaluated by Malvern. From the obtained particle size, it indicated that the particle size of QCT in QCT-MMs was widely distributed. The polydispersity index (PDI) for QCT-MMs was found in the range of ~1.000, which indicates its narrow range of distribution. Zeta potential (ζ) is one of the significant properties of the particle, which determine the surface charges surrounding the particles. It is a potential indicator of the physical stability of particles in a liquid dispersion. Zeta potential value greater than (>30 mV), demonstrates exceptional stability in the formulations. Fig. 7 shows the zeta potential of prepared QCT-MMs. In the current study, the zeta potential value for QCT-MMs as evaluated by Malvern was observed to be ~-99.2 mV. So, the prepared QCT-MMs formulation with obtained low particle size, lower PDI, and Negative zeta potential values could be attributable to the better physical stability of QCT-MMs [29, 30].

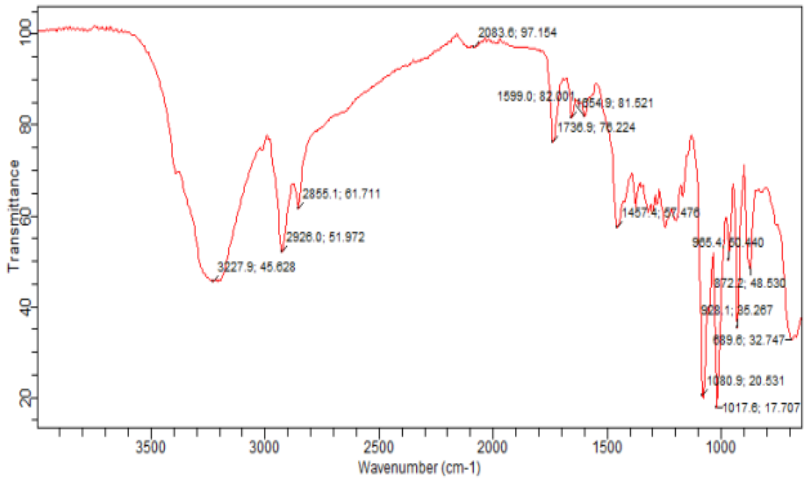

Fig. 5: FT-IR of QCT-MMs

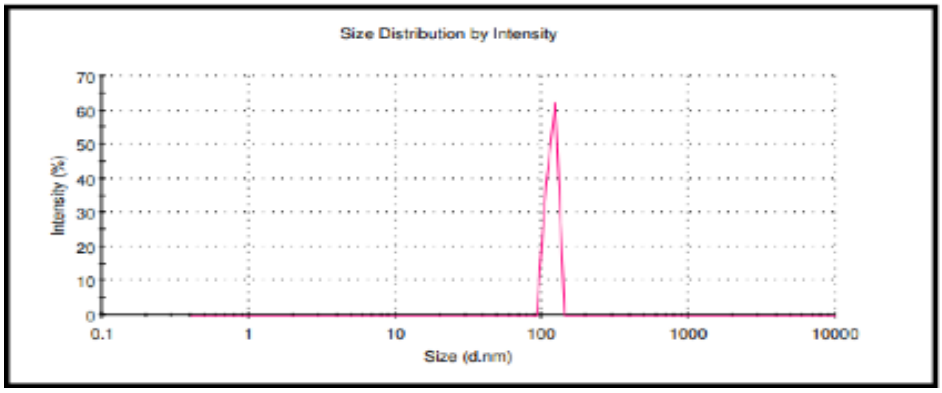

Fig. 6: Particle size distribution of QCT-MM

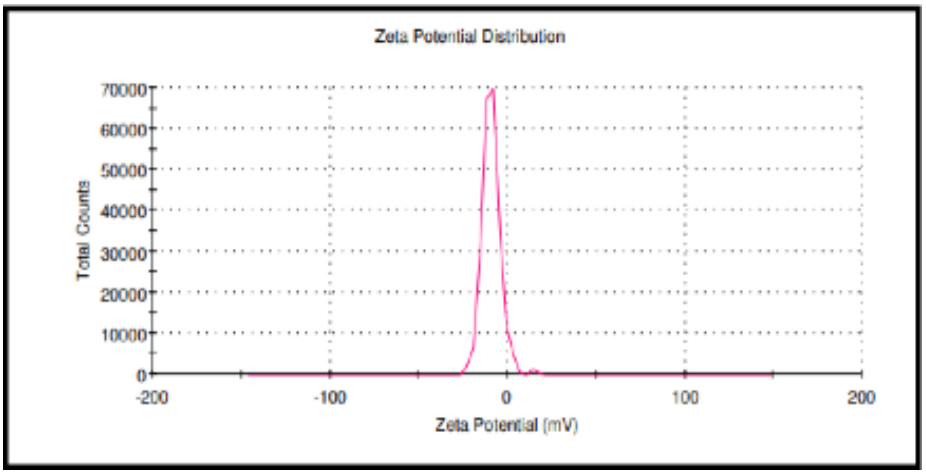

Fig. 7: Zeta potential of QCT-MMs

Powder X-ray diffract study

The crystalline nature of the synthesized QCT-MMs was confirmed by the X-ray diffraction analysis. In fig. 8, fig. 9, fig. 10, fig. 11 and fig. 12 shows the PXRD pattern of Lipoid S-75, Lipoid S-100, and QCT, respectively. The unassigned peaks could be due to the crystallization of the bioorganic phase that occurs on the surface of the QCT-MMs. The PXRD pattern indicates that the QCT-MMS are crystalline [31].

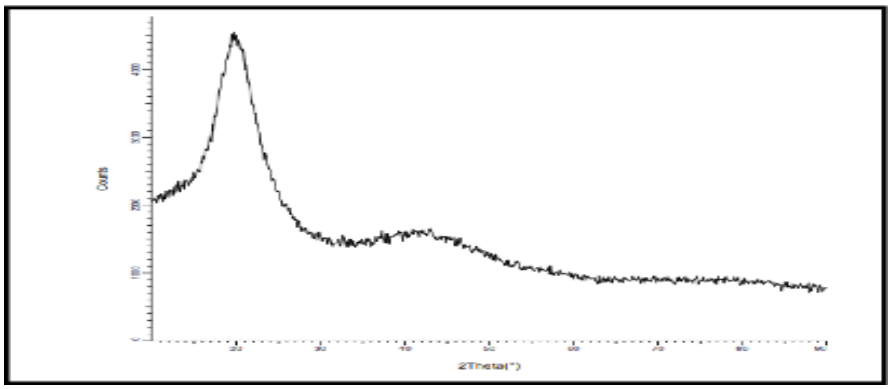

Fig. 8: PXRD of LS-75

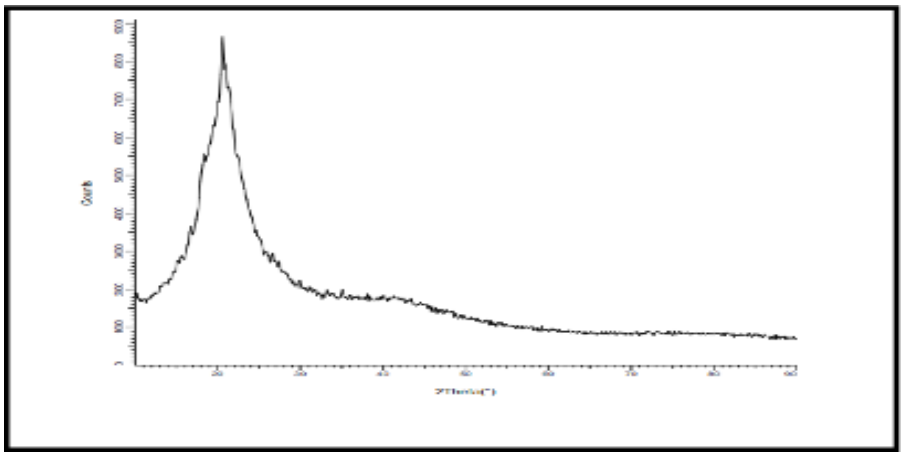

Fig. 9: PXRD of LS-100

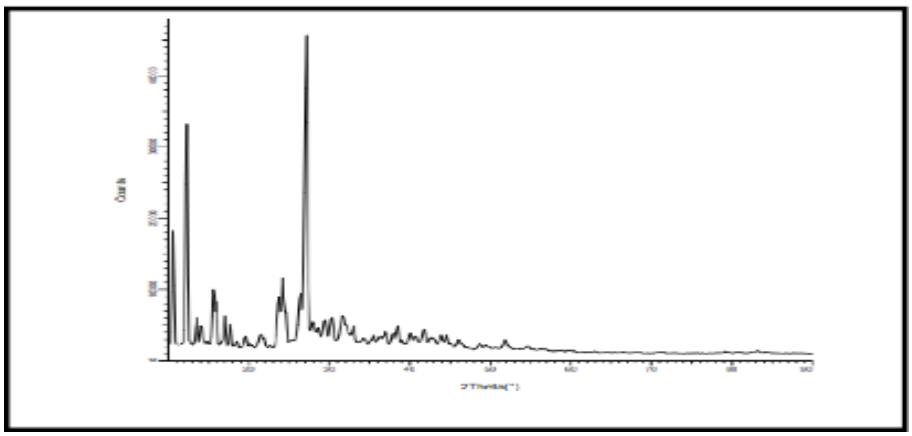

Fig. 10: PXRD of QCT

***In vitro* drug dissolution**

The *in vitro* QCT release from the QCT-MMs was studied by dialysis method using PBS with 0.5% Tween 80 as release medium to get the sink condition PBS (pH 6.8) at 37 °C. After 8 h, the percentage of QCT released from QCT and QCT-MMs was 12 % and 30 %; as shown in fig. 13 QCT showed sustained release behavior from QCT-MMs. More than 90 % of QCT was released from free QCT within 12 h, while the release of QCT from QCT-MMs was sustained up to 72 h.

Due to the insolubility of UA in water, a free QCT solution was prepared by dissolving QCT in Propylene glycol. The result indicated that the core stably accommodated the hydrophobic drug resulting in controlled drug release [32].

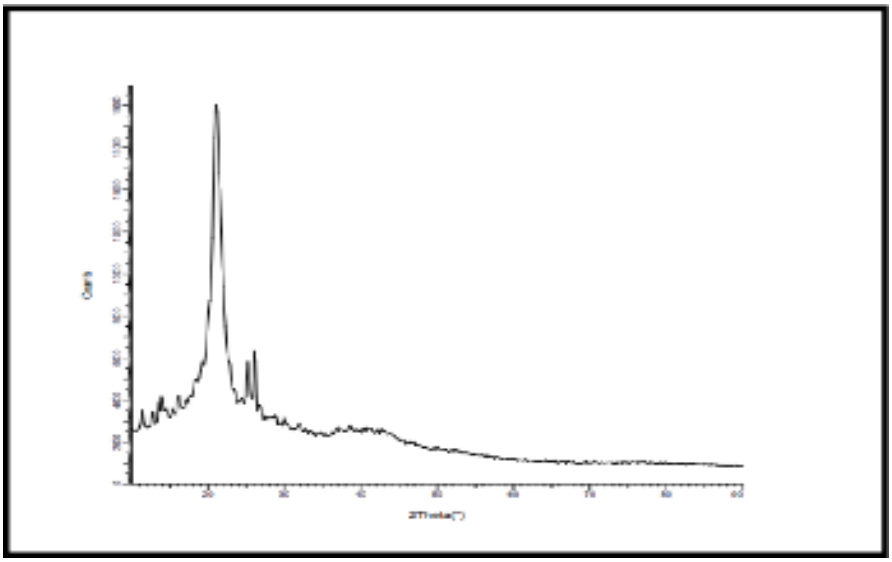

Fig. 11: PXRD of physical mixture

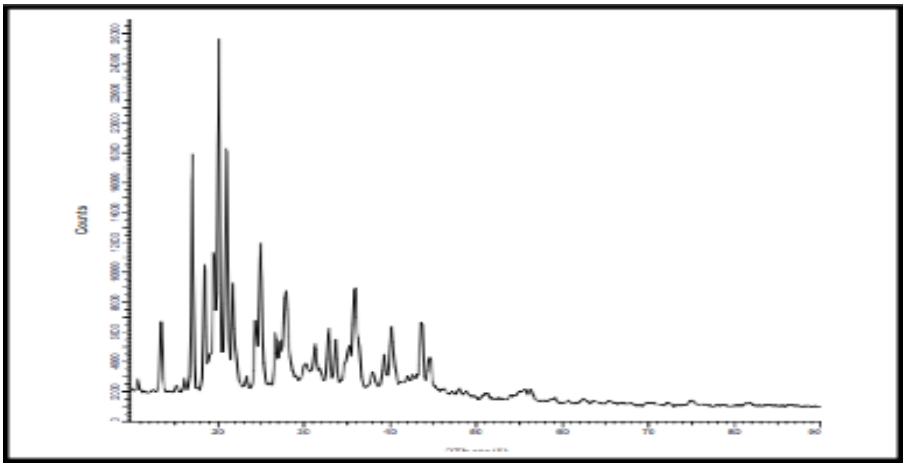

Fig. 12: PXRD of QCT-MMs

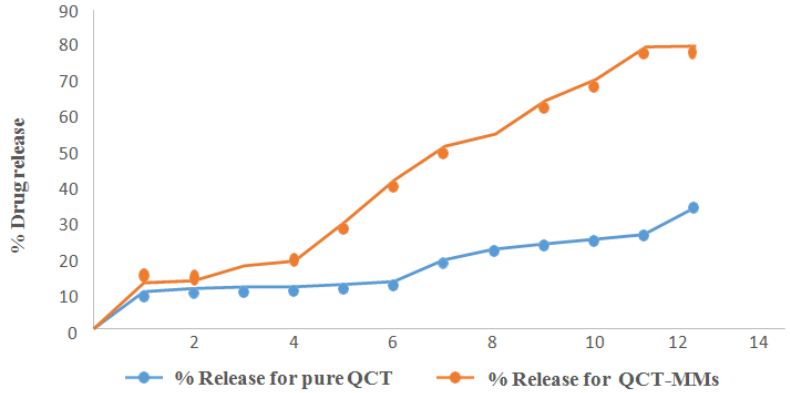

Fig. 13: QCT release kinetics from free QCT in propylene glycol, QCT-MMs in PBS (pH 6.8) at 37 °C. Data represents mean (n=3)

TEM

The morphology of the selected QCT-MMs formulations was observed using high-resolution TEM. Fig. 14 shows the TEM images of QCT-MMs, where the micelles exhibited relatively regular dark stained shapes appearing more or less spherical or spheroid. Their diameters appeared to be lower than the results obtained by the PS experiment, which was mainly due to water evaporation in the TEM experiments. The micelles were examined in the dry state and lacked a hydration layer, thus resulting in their shrinkage and smaller. It was also observed that QCT-MMs fig. 14 was dispersed and more populated in the field. This finding is from a previous study reporting a subsequent increase in spherical micelles as a result of increased poloxamer content [33].

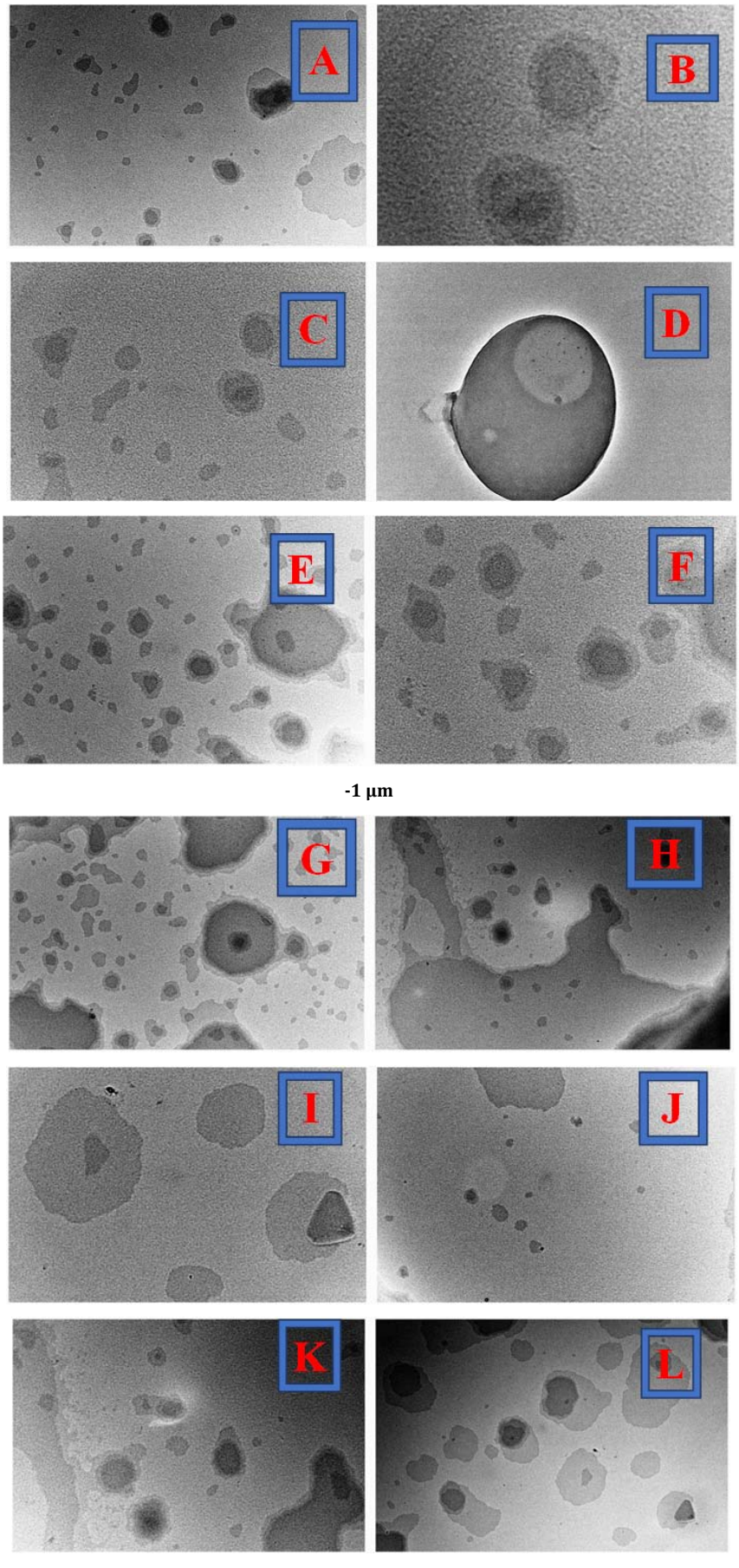

Fig. 14: TEM images of QCT-MMs 1 µm

CONCLUSION

QCT is the BCS class II drug, which is a potent antioxidant and anti-cancer agent, has low solubility parameters while preparing dosage forms. QCT-MMs is the finest one because it is easiest as well as simplest to formulate and inexpensive concerning others and great patient compliance as compared to others in the treatment of cancer. From the above study, it can be concluded that QCT-MMs help to enhance the solubility of the quercetin in addition to enhancing the stability of the formulation. QCT-MMs can be easily administered through suitable dosage forms due to their firmness with potent activity in the treatment of cancer and thus improving patient compliance. The gum-loaded QCT-MMs can be easily administered parenterally due to their less viscous nature and thus improving patient compliance. Also from the above study, it was concluded that 97.65% of drug release was obtained after 8 h.

This system has several advantages due to the use of lipids in the formulation, such as high tolerability, controlled release, protection of the drug against harsh exposure, and reducing side effects that can be caused. This study indicated that the composition of the formulation and the technique of producing QCT-MMs affected the physicochemical properties of the QCT-MMs and the release profile of the QCT.

ACKNOWLEDGEMENT

All the authors of this manuscript express their sincere thanks to the Dr. Anil M. Pethe, Principal, Datta Meghe College of Pharmacy, Wardha. It is a great pleasure to acknowledge my immense respect and deep gratitude to Dr. Darshan Telange. Assistant professor, Datta Meghe College of Pharmacy, Wardha. for technical and writing support.

FUNDING

Nil

AUTHORS CONTRIBUTIONS

All the authors contributed equally.

CONFLICTS OF INTERESTS

There is no conflict of interest among authors.

REFERENCES

1. Hemant K, Abhay R, Praveen S, Swati U, Hemanth KS. Cancer nanotechnology: nanoparticulate drug delivery for the treatment of cancer. Int J Pharm Pharm Sci 2022;7(3):40-6.
2. Zheng G, Chen J, Li H, Glickson JD. Rerouting lipoprotein nanoparticles to selected alternate receptors for the targeted delivery of cancer diagnostic and therapeutic agents. Proc Natl Acad Sci USA. 2005;102(49):17757-62. doi: 10.1073/pnas.0508677102, PMID 16306263.
3. Molavi O, Ma Z, Mahmud A, Alshamsan A, Samuel J, Lai R. Polymeric micelles for the solubilization and delivery of STAT3 inhibitor cucurbitacins in solid tumors. Int J Pharm. 2008;347(1-2):118-27. doi: 10.1016/j.ijpharm.2007.06.032, PMID 17681440.
4. Kazunori K, Yokoyama M, Masayuki Y, Teruo O, Yasuhisa S. Block copolymer micelles as vehicles for drug delivery. J Control Release. 1993;24(1-3):119-32. doi: 10.1016/0168-3659(93)90172-2.
5. Kim S, Shi Y, Kim JY, Park K, Cheng JX. Overcoming the barriers in micellar drug delivery: loading efficiency, *in vivo* stability, and micelle–cell interaction. Expert Opin Drug Deliv. 2010;7(1):49-62. doi: 10.1517/17425240903380446, PMID 20017660.
6. Xiong XB, Falamarzian A, Garg SM, Lavasanifar A. Engineering of amphiphilic block copolymers for polymeric micellar drug and gene delivery. J Control Release. 2011;155(2):248-61. doi: 10.1016/j.jconrel.2011.04.028, PMID 21621570.
7. Senthil Kumar Raju. Biogenic synthesis of copper nanoparticles and their biological applications: an overview. Int J Pharm Pharm Sci. 2022;14(3):8-26. doi:10.22159/ijpps.2022v14i3.43842.
8. Cabral H, Matsumoto Y, Mizuno K, Chen Q, Murakami M, Kimura M. Accumulation of sub-100 nm polymeric micelles in poorly permeable tumours depends on size. Nat Nanotechnol. 2011;6(12):815-23. doi: 10.1038/nnano.2011.166, PMID 22020122.
9. Khan YY, Suvarna V. Liposomes containing phytochemicals for cancer treatment-an update. Int J Curr Pharm Sci. 2017;9(1). doi: 10.22159/ijcpr.2017v9i1.16629.
10. Telange DR, Patil AT, Pethe AM, Fegade H, Anand S, Dave VS. Formulation and characterization of an apigenin-phospholipid phytosome (APLC) for improved solubility, *in vivo* bioavailability, and antioxidant potential. Eur J Pharm Sci. 2017;108:36-49. doi: 10.1016/j.ejps.2016.12.009. PMID 27939619.
11. Sivapriya V, Ponnarmadha S, Azeezand NA, Sudarshanadeepa V. Novel nanocarriers for ethnopharmacological formulations. Int J App Pharm. 2018;10(4):26-30. doi: 10.22159/ijap.2018v10i4.26081.
12. Senthil Kumar Raju. Biogenic synthesis of copper nanoparticles and their biological applications: an overview. Int J Pharm Pharm Sci. 2022;14(3):8-26. doi:10.22159/ijpps.2022v14i3.43842.
13. Gautam A, Bepler G. Suppression of lung tumor formation by the regulatory subunit of ribonucleotide reductase. Cancer Res. 2006;66(13):6497-502. doi: 10.1158/0008-5472.CAN-05-4462, PMID 16818620.
14. Merlo LMF, Pepper JW, Reid BJ, Maley CC. Cancer as an evolutionary and ecological process. Nat Rev Cancer. 2006;6(12):924-35. doi: 10.1038/nrc2013, PMID 17109012.
15. Sub K, Park W, Hu J, Han Y, Na K. Biomaterials a cancer-recognizable MRI contrast agents using pH-responsive polymeric micelle. Biomaterials. 2014;35(1):337-43. https://doi.org/10.1016/j.biomaterials.2013.10.004
16. Gao Y, Li Z, Xie X, Wang C, You J, Mo F. Dendrimeric anticancer prodrugs for targeted delivery of ursolic acid to folate receptor-expressing cancer cells: synthesis and biological evaluation. Eur J Pharm Sci. 2015;70:55-63. doi: 10.1016/j.ejps.2015.01.007. PMID 25638419.
17. Lipinski CA, Lombardo F, Dominy BW, Feeney PJ. Experimental and computational approaches to estimate solubility and permeability in drug discovery and development settings. Adv Drug Deliv Rev. 2001;46(1-3):3-26. doi: 10.1016/s0169-409x(00)00129-0. PMID 11259830.
18. B Jeevana Jyothi. Development and *in vitro* evaluation of phytosomes of naringin. Asian J Pharm Clin Res. 2019;12(9):252-6. doi: 10.22159/ajpcr.2019.v12i9.34798.
19. Giordano KF, Jatoi A. The cancer anorexia/weight loss syndrome: therapeutic challenges. Curr Oncol Rep. 2005;7(4):271-6. doi: 10.1007/s11912-005-0050-9, PMID 15946586.
20. Park JH, Lee S, Kim J, Park K, Kim K, Kwon IC. Polymeric nanomedicine for cancer therapy. Prog Polym Sci. 2008;33(1):113-37. doi: 10.1016/j.progpolymsci.2007.09.003.
21. Kumari A, Yadav SK, Yadav SC. Biodegradable polymeric nanoparticles based drug delivery systems. Colloids Surf B Biointerfaces. 2010;75(1):1-18. doi: 10.1016/j.colsurfb.2009.09.001, PMID 19782542.
22. Schoellhammer CM, Blankschtein D, Langer R. Skin permeabilization for transdermal drug delivery: recent advances and future prospects. Expert Opin Drug Deliv. 2014;11(3):393-407. doi: 10.1517/17425247.2014.875528, PMID 24392787.
23. Donnelly RF, Singh TRR, Garland MJ, Migalska K, Majithiya R, McCrudden CM. Hydrogel-forming microneedle arrays for enhanced transdermal drug delivery. Adv Funct Mater. 2012;22(23):4879-90. doi: 10.1002/adfm.201200864, PMID 23606824.
24. Brambilla D, Luciani P, Leroux JC. Breakthrough discoveries in drug delivery technologies: the next 30 y. J Control Release. 2014;190:9-14. doi: 10.1016/j.jconrel.2014.03.056. PMID 24794899.
25. Salam AE WH, El-Helaly SN. Preparation of novel phospholipid-based sono complexes for improved intestinal permeability of rosuvastatin. Int J Pharm. 2018;548(1):375-84. doi: 10.1016/j.ijpharm.2018.07.005.
26. Yang X, Hou Y, Gong T, Sun L, Xue J, Guo Y. Concentration-dependent rheological behavior and gelation mechanism of high acyl gellan aqueous solutions. Int J Biol Macromol. 2019;131:959-70. doi: 10.1016/j.ijbiomac.2019.03.137, PMID 30910680.

27. Zoratto N, Grillo I, Matricardi P, Dreiss CA. Supramolecular gels of cholesterol-modified gellan gum with disc-like and worm-like micelles. J Colloid Interface Sci. 2019;556:301-12. doi: 10.1016/j.jcis.2019.08.057, PMID 31454622.
28. Hsu MF, Tyan YS, Chien YC, Lee MW. Hyaluronic acid-based nano-sized drug carrier-containing Gellan gum microspheres as potential multifunctional embolic agent. Sci Rep. 2018;8(1):731. doi: 10.1038/s41598-018-19191-7. PMID 29335649.
29. Mandal A, Bisht R, Rupenthal ID, Mitra AK. Polymeric micelles for ocular drug delivery: from structural frameworks to recent preclinical studies. J Control Release. 2017;248:96-116. doi: 10.1016/j.jconrel.2017.01.012, PMID 28087407.
30. Khalid A, Zia M. Recent trends on gellan Gum blends with natural and synthetic polymers: a review. Int J Biol Macromol. 2018;109:1068-87. doi: 10.1016/j.ijbiomac.2017.11.099.
31. Duan Y, Cai X, Du H, Zhai G. Novel in situ gel systems based on P123/TPGS mixed micelles and gellan gum for ophthalmic delivery of curcumin. Colloids Surf B Biointerfaces. 2015;128:322-30. doi: 10.1016/j.colsurfb.2015.02.007. PMID 25707750.
32. Maiti S, Chakravorty A, Chowdhury M. Gellan co-polysaccharide micellar solution of budesonide for allergic anti-rhinitis: an *in vitro* appraisal. Int J Biol Macromol. 2014;68:241-6. doi: 10.1016/j.ijbiomac.2014.05.003. PMID 24820153.
33. Arrigo GD, Navarro G, Di C, Matricardi P, Torchilin V. Gellan gum nano hydrogel containing anti-inflammatory and anticancer drugs: a multi-drug delivery system for combination therapy in cancer treatment. Eur J Pharm Biopharm. 2013;11:1-9. doi: 10.1016/j.ejpb.2013.11.001.